Intelligent Flight State Identification of a Self-Sensing Wing through Neural Network Modelling

XI CHEN, FOTIS KOPSAFTOPOULOS, HAILIN CAO and FU-KUO CHANG

ABSTRACT

With the development of micro-fabrication techniques, multi-functional sensor networks have been created with many micro-sensor nodes for various functions. An UAV wing is integrated with a stretchable sensor network including piezoelectric transducer, strain gauge and resistance temperature detector embedded near the wing surface and this novel design intends to equip the wing with the self-sensing capability similar to bird feathers. One of the main challenges of the state-of-the-art research is how to make the wing aware its flight states in real-time through large amount of sensing signals. Features are extracted and further selected for neural network modelling. Both classic neural network and deep belief network are proposed respectively to map the relationship from the sensing data to physical flight states and compare the identification accuracy with each other. The simulation results show a relatively high identification accuracy of the proposed methods, enabling new perspectives in developing intelligent self-awareness capabilities for next generation smart wings.

INTRODUCTION

Identification of flight states lays the foundation for flight control and air vehicle health management. Accurate grasp of air dynamic characteristics can help recover the aircraft when it draws near to stall or flutter situation, which ensures flight safety. Currently, the flight state parameters are collected based on traditional sensors amounted on different locations of the aircraft, e.g. pitot tube in front of the nose for air speed measurement, transducer amounted on the wing for angle of attack detection [1]. With the fast development of sensing technology, sensors become lighter and thinner. Various sensors

Stanford University, 450 Serra Mall, Stanford, CA 94305, U.S.A.

can constitute a multi-functional sensor network which is able to be embedded into the structure without compromising structural integrity [2]. Inspired by bird's feathers that can feel surrounding aerodynamic force, NASA proposed a design concept called 'fly-by-feel' for next generation aircraft [3]. Specifically, it intends to equip the aircraft with a self-sensing capability via an integration of multiple micro-sensors with the wing structure. This smart wing will be able to 'feel', 'think', and 'react' in real time based on high-resolution state-sensing capabilities, allowing for superior performance in complex dynamic environments through autonomous control as well as life-cycle health monitoring. Compared with the current wing structure, it has the following advantages [4]: 1) structural complexity reduction by saving the efforts of large sensors installation, 2) structural health monitoring through the embedded multi-functional sensor network, 3) extreme conditions investigation and prevention for flight safety improvement, 4) autonomous flight control for real-time optimum decision-making, 5) maintenance cost reduction and structural design optimization.

One of the self-sensing solutions proposed by Structure and Composite Laboratory (SACL) at Stanford is a novel stretchable sensor network in the composite wing as shown in Figure 1.

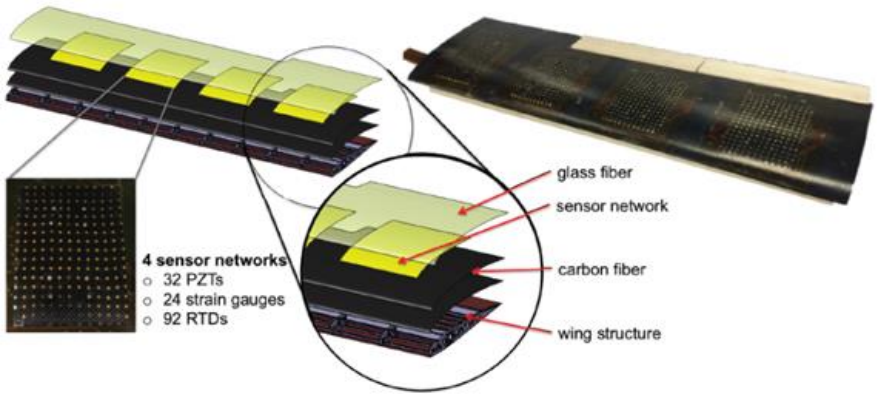

Figure 1. multi-functional sensor network developed by SACL.

This particular design includes integrated strain gauge, resistance temperature detector (RTD), and piezoelectric transducer (PZT) monolithically distributed in the layup of the composite UAV wing [4]. Strain gauge is used to measure the wing strain distribution and identify the potential dangerous area. RTD detects the temperature distribution in order to provide the temperature compensation [5]. PZT has both active and passive measurements. For active mode, it can be used for damage detection and structural health monitoring while in passive mode, the wing structural vibration during flying can be captured to reflect the air dynamic characteristics [6].

The wing tunnel experiments of the first-generation self-sensing wing were conducted at various flight speeds and angles of attack, and considerable amount of signals from the sensor network were generated. One of the main challenges of the state-of-the-art research is how to make the wing self-aware its flight states in real-time. Therefore, the objective of this paper is to addresses the intelligent flight identification problem via establishing the mapping relationship from the sensing signal space to the practical operating space. Vibration signals from PZT near the wing tip are collected and 16 experimental flight

states (combinations of air speed and angle of attack) are selected for classification in which model two different neural network techniques are investigated respectively.

FEATURE EXTRACTION AND SELECTION

Each vibration signal sample contains repeated patterns and the first step is to obtain useful features that can be used as model input. In this analysis, totally 37 feature parameters are extracted from both time-domain and frequency-domain as listed in TABLE I. The time domain features can be divided into two parts. The first part includes 11 commonly used statistical features: mean, standard deviation, skewness, kurtosis, variance, root mean square, peak, etc. and the second part includes un-dimensional features such as crest factor, shape factor as well as a series of normalized central moments [7]. The frequency domain features are obtained from Fast Fourier Transform (FFT) covering typical statistical characters as mean frequency, frequency center, root mean square frequency, etc. Their physical meanings are presented as follows for better understanding [8]. t_1-t_{11} may reflect the vibration amplitude and energy in the time domain. t_{12}-t_{24} may represent the time series distribution of the signal in time domain. f_1 may indicate the vibration energy in the frequency domain. $f_{2\text{-}4}$, f_6, $f_{10\text{-}13}$ may describe the convergence of the spectrum power. f_5, $f_{7\text{-}9}$ may show the position change of the main frequency.

TABLE I. EXTRACTED FEATURES FROM BOTH TIME-DOMAIN AND FREQUENCY-DOMAIN

Time domain feature parameters		Frequency domain feature parameters	
$t_1=\frac{\sum_{n=1}^{N}x(n)}{N}$	Un-dimensional	$f_1=\frac{\sum_{k=1}^{K}y(k)}{N}$	$f_{12}=\frac{\sum_{k=1}^{K}(fr_k-f_5)^4y(k)}{K\cdot f_6^{\,4}}$
$t_2=\sqrt{\frac{\sum_{n=1}^{N}(x(n)-t_1)^2}{N}}$	$t_{12}=\frac{t_9}{t_6}$	$f_2=\frac{\sum_{k=1}^{K}(y(k)-f_1)^2}{K}$	$f_{13}=\frac{\sum_{k=1}^{K}\sqrt{\lvert fr_k-f_5\rvert}y(k)}{K\sqrt{f_6}}$
$t_3=\frac{\sum_{n=1}^{N}(x(n))^3}{N}$	$t_{13}=\frac{t_6}{t_8}$	$f_3=\frac{\sum_{k=1}^{K}(y(k)-f_1)^3}{K(\sqrt{f_2})^3}$	where $y(k)$ is a spectrum for $k=1,2,\ldots,K$, K is the number of spectrum components; fr_k is the frequency value of the k^{th} spectrum line
$t_4=\frac{\sum_{n=1}^{N}(x(n))^4}{N}$	$t_{14}=\frac{t_9}{t_8}$	$f_4=\frac{\sum_{k=1}^{K}(y(k)-f_1)^4}{K\cdot f_2^{\,2}}$	
$t_5=\frac{\sum_{n=1}^{N}(x(n)-t_1)^2}{N}$	$t_{15}=\frac{t_9}{t_7}$	$f_5=\frac{\sum_{k=1}^{K}(fr_k\cdot y(k))}{\sum_{k=1}^{K}y(k)}$	
$t_6=\sqrt{\frac{\sum_{n=1}^{N}(x(n))^2}{N}}$	$t_{16}=\frac{t_3}{t_6^{\,3}}$	$f_6=\sqrt{\frac{\sum_{k=1}^{K}(fr_k-f_5)^2y(k)}{K}}$	
$t_7=\left(\frac{1}{N}\sum_{n=1}^{N}\sqrt{\lvert x(n)\rvert}\right)^2$	$t_{17}=\frac{t_4}{t_6^{\,4}}$	$f_7=\sqrt{\frac{\sum_{k=1}^{K}fr_k^{\,2}y(k)}{\sum_{k=1}^{K}y(k)}}$	
$t_8=\frac{\sum_{n=1}^{N}\lvert x(n)\rvert}{N}$	$t_{18}=\frac{\sum_{n=1}^{N}(x(n)-t_1)^3}{N\cdot t_2^{\,3}}$	$f_8=\sqrt{\frac{\sum_{k=1}^{K}fr_k^{\,4}y(k)}{\sum_{k=1}^{K}fr_k^{\,2}y(k)}}$	
$t_9=\max(x(n))$	…	$f_9=\frac{\sum_{k=1}^{K}fr_k^{\,2}y(k)}{\sqrt{\sum_{k=1}^{K}y(k)\sum_{k=1}^{K}fr_k^{\,4}y(k)}}$	
$t_{10}=\min(x(n))$	$t_{24}=\frac{\sum_{n=1}^{N}(x(n)-t_1)^9}{N\cdot t_2^{\,9}}$	$f_{10}=\frac{f_6}{f_5}$	

$t_{11} = t_{10} - t_{11}$	where $x(n)$ is a signal series for n=1, 2,…N, N is the number of data points	$f_{11} = \frac{\sum_{k=1}^{K} (fr_k - f_5)^3 y(k)}{K \cdot f_6^3}$	

Although the above 37 features may identify flight conditions from various aspects, not all of them should be fed into the classifier since their importance degrees are different. Salient features providing sound states identification capability should be remained while irrelevant features which have little effect in classification should be removed in order to reduce the input dimensionality. Thus, some distance evaluation technique should be developed to selected the salient feature set from the whole feature pool. Herein, an improved evaluation algorithm is applied including the following steps as shown in Figure 2 [9].

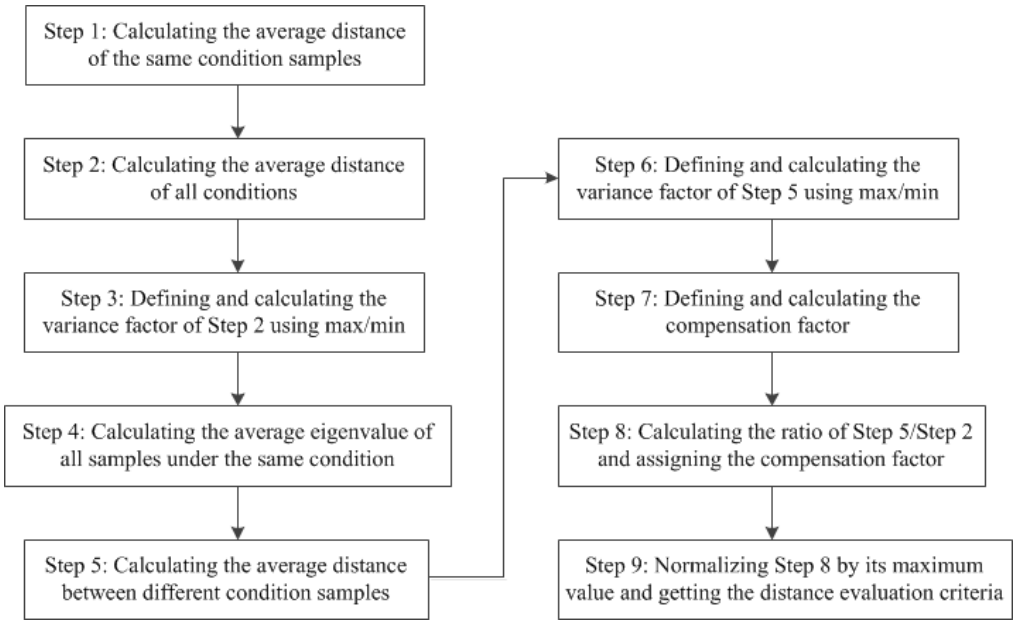

Figure 2. Distance evaluation algorithm.

After the above procedures, 12 features are finally selected which have the highest important degrees. A visualization of some features is shown in Figure 3.

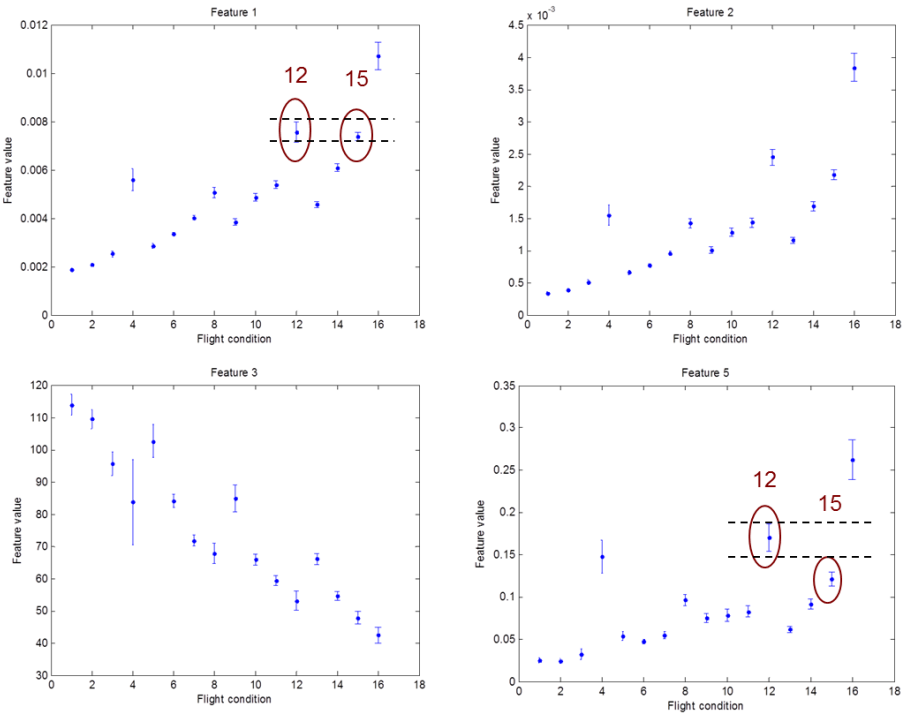

Figure 3. Selected features visualization.

Take Feature 1 and Feature 5 for example. Overall, Feature 1 have the best classification ability. However, it is insufficient to distinguish between flight condition 12 and 15 since statistical values overlap with each other. Instead, Feature 5 is able to identify these two flight states although it has limited capabilities for other flight states. This implies that a combination of different feature can achieve better identification result and the next step is to establish proper neural networks to learn this complex combination mechanism.

NEURAL NETWORK METHODOLOGIES

SUPERFICIAL NEURAL NETWORK

The first neural network uses a classic superficial configuration with three layers: an input layer, a hidden layer and an output layer. The training procedure can be divided into the feed forward and back propagation. Once the weights W and bias b of the network are initialized, the feed forward from input to output includes linear calculation for layer l+1 as

$$z^{(l+1)} = W^{(l)}x + b^{(l)} \tag{1}$$

and activation function as

$$a^{(l+1)} = f\left(z^{(l+1)}\right) = f(W^{(l)}x + b^{(l)}) \tag{2}$$

The final output is expressed as

$$h_{W,b}(x) = a^{(3)} = f(z^{(3)}) \tag{3}$$

Then a loss function $L(\theta)$ is defined to measure the difference between the forwarded output and the target y. It should be noted that loss functions can be various form depending on different training purposes.

The back-propagation step is used to adjust the network parameters (weights W and bias b) through gradient descent calculation. The general calculation form from output to input at each iteration is expressed as

$$W^{(l)} = W^{(l)} - \alpha \frac{\partial L}{\partial W^{(l)}} \tag{4}$$

$$b^{(l)} = b^{(l)} - \alpha \frac{\partial L}{\partial b^{(l)}} \tag{5}$$

where α is the learning rate.

Accordingly, the network parameters will be updated for each forward and backward calculation and the objective of the training is to minimize the loss function. If the loss function is convex, it will finally reach a global minimum, otherwise, it is easy to stuck at some local minimal bottom. Therefore, some optimization methods such as genetic algorithm is often applied to initialize the network parameters in avoid of local minimum [10]. Another problem with the traditional neural network is that gradients become spars or even diffuse with increasing layers, which restricts the layers at small numbers.

DEEP BELIEF NETWORK

Deep Belief Network (DBN) is a generative graphic model composed of multiple layers of hidden nodes with connections between each layer but no connections within each layer [11]. As one of the deep learning methods, DBN has achieved successful applications in many areas such as speech processing and image recognition. It overcomes the gradients diffusion problem of traditional back-propagation network by applying a layer-wised training approach.

DBN is constructed by stacking a series of Restricted Boltzmann Machines (RBM). RBM can be regarded as an undirected graph including a visible layer for observed data and a hidden layer for feature detection. The energy function is defined as

$$E(v,h \mid \theta) = -\sum_{i=1}^{n} a_i v_i - \sum_{j=1}^{m} b_j h_j - \sum_{i=1}^{n}\sum_{j=1}^{m} v_i W_{ij} h_j, \quad \theta = \{W_{ij}, a_i, b_j\} \tag{6}$$

where v, h indicate node values in the visible layer and the hidden layer, W is the weights between the visible layer and hidden layer, a,b denote the bias of the visible layer and the hidden layer. θ is the set of parameters including W, a and b.

Given the parameters θ, the joint probability distribution based on the energy function is

$$P(v,h \mid \theta) = \frac{e^{-E(v,h|\theta)}}{Z(\theta)}, \quad Z(\theta) = \sum_{v,h} e^{-E(v,h|\theta)} \tag{7}$$

and the marginal probability assigned to the visible node v is

$$P(v \mid \theta) = \frac{\sum_{h} e^{-E(v,h|\theta)}}{Z(\theta)}, \quad Z(\theta) = \sum_{v,h} e^{-E(v,h|\theta)} \tag{8}$$

The objective of the network training is to find the maximum value for the defined loss function expressed as

$$\theta^* = \arg\max_{\theta} \ell(\theta) = \arg\max_{\theta} \sum_{v} \log P(v \mid \theta) \tag{9}$$

Learning is conducted by an approximation to the gradient of the loss function using 'Contrastive Divergence' method. For details, please refer to [11].

The training process can be divided into two steps. The first step is to train each RBM from input to final output in an unsupervised way. The output of each RBM will be taken as the input into the next RBM layer while the parameters of the previous layer fix. This layer-by-layer training can be regarded as a feature learning process, each output is an advanced representation of the previous input data. All network parameters are initialized after completion of the layer-wised forward learning.

The second step is to use back propagation from the final output to input throughout the network with sample targets. This supervised training step further adjusts the network parameters globally which is called fine-tune.

MODELLING AND RESULTS

BPN MODELLING AND RESULTS

A 3-layer back-propagation network (BPN) is established with selected 12 features as input and 16 flight states as output. Logistic regression is used in the output layer as binary classifier for each output node. The model structure is shown in Figure 4. If a new signal is input, the BPN is expected to output the exact flight state by activating one of the output node with value 1.

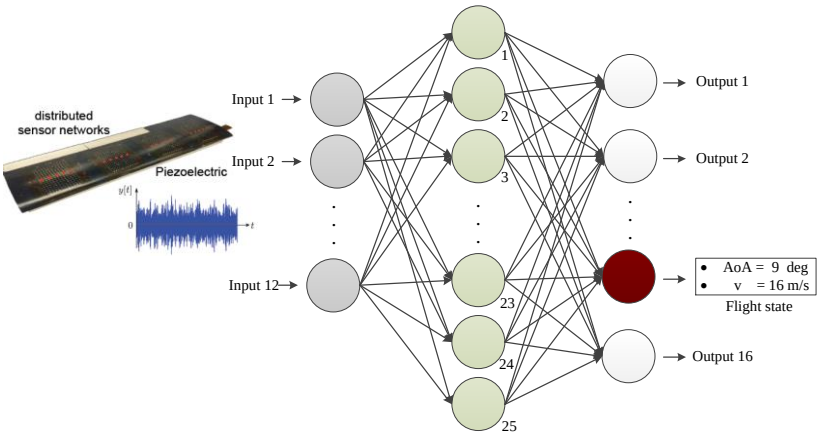

Figure 4. BPN for flight identification.

The selection of number of hidden nodes plays an important role in network performance, but there is no universal method. This analysis examines and the final identification accuracy against a series of hidden node numbers and the results are

displayed in Figure 5. Considering the stochastic characteristics of each simulation process, every situation was run 20 times to obtain the average value. Also, it is noted that genetic algorithm is applied for initialization of the network parameters to avoid local minimum.

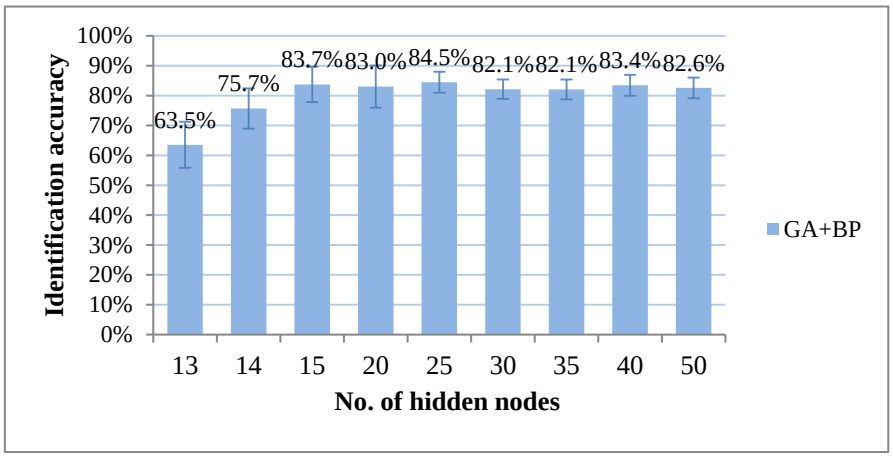

Figure 5. Flight identification accuracy against No. of hidden nodes.

It can be seen that the BPN with 25 hidden nodes has the highest identification accuracy (84.5%).

DBN MODELLING AND RESULTS

A 5-layer deep belief network (DBN) is developed with 3 RBMs stacked progressively and the output layer uses Softmax regression as the multi-classifier. The diagram of the network structure is shown in Figure 6 with 12 input features and 16 output flight states.

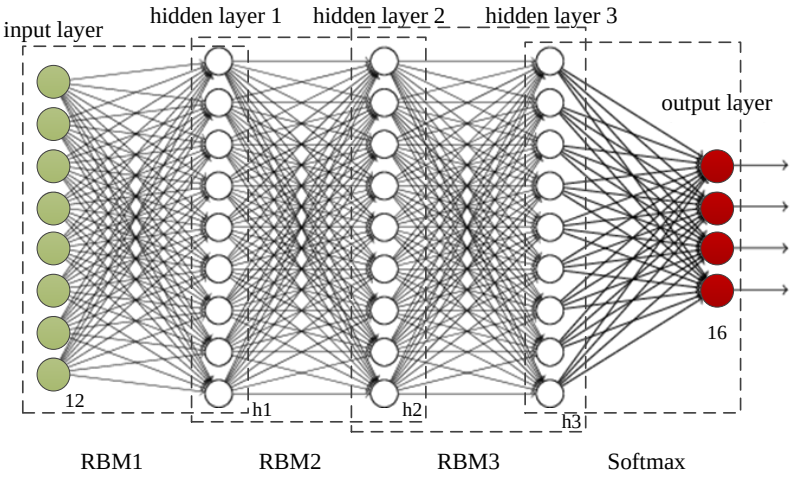

Figure 6. Diagram of the DBN.

Four types of DBN configuration with two different settings of 3 hidden layers in each type are investigated and compared. Each simulation was conducted 20 times and the identification results are listed in TABLE II and visualized in Figure 7.

TABLE II. IDENTIFICATION ACCURACY FOR VARIOUS DBN STRUCTURES

DBN type	DBN structure	Identification accuracy
Increasing type	12 - 20 - 40 - 60 - 16	87.81%
	12 - 36 - 72 - 108-16	87.22%
Decreasing type	12 - 80 - 60 - 40 - 16	86.68%
	12 -108 - 72 - 36 - 16	86.09%
Constant type	12 - 40 - 40 - 40 - 16	89.40%
	12 - 80 - 80 - 80 - 16	85.13%
Mix type	12 - 40 - 80 - 40 - 16	86.19%
	12 - 40 - 40 - 80 - 16	88.59%

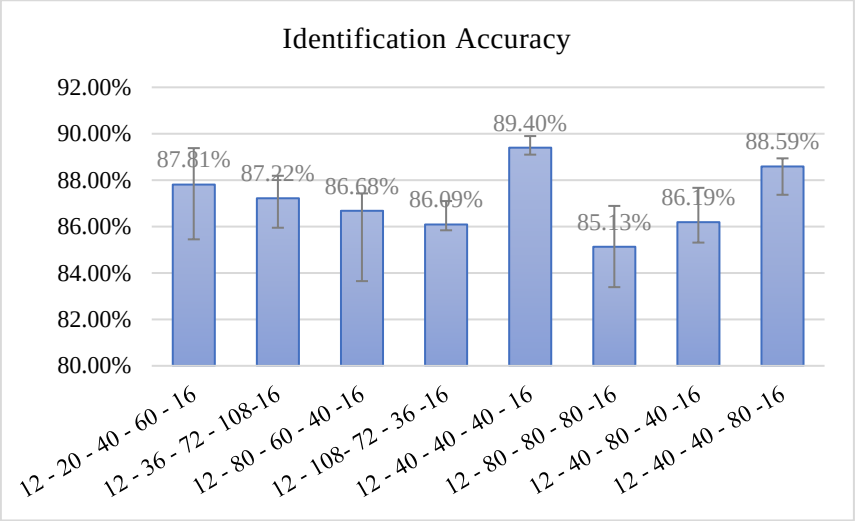

Figure 7. Identification accuracy of different DBN structures.

It can be seen from Table 2 that overall, DBN achieves higher identification accuracy compared with previous BPN, and among all types, constant-layer structure (12-40-40-40-16) has the highest flight identification accuracy which is up to 89.4%.

CONCLUSION

In this study, special emphasis is given to the vibration signal obtained from piezoelectric sensors and two neural network frameworks are proposed for flight states identification. A wide collection of various statistical features was extracted from both time-domain and frequency domain and a set of most silent features were further selected based on an improved distance evaluation algorithm. The first model is a 3-layer back-propagation network with logistic regression as output while the second model is a 5-layer deep belief network with softmax regression as output. The simulation results show that both methods can achieve relatively sound identification accuracy and networks with more layers and advanced learning algorithms have higher precision, demonstrating the superior performance of the deep neural network. This research enables new perspectives in developing intelligent self-awareness capabilities for next generation smart wings.

REFERENCES

1. Nelson R. C. 1998. “Flight stability and automatic control,” *WCB/McGraw Hill New York*, New York.

2. Lanzara G., Feng J., Chang F-K. 2010. “Design of micro-scaled highly expandable networks of polymer based substrates for macro-scale applications,” *Smart Mater Struct*., 19(4): 045013.

3. The National Aeronautics and Space Administration. 2011. “Fly-By-Feel Systems Represent The Next Revolution In Aircraft Controls,” *In. The Dryden X-Press AERONATIONS*.

4. Kopsaftopoulos F., Nardari R., Li Y., Wang P, Ye B., Chang F-K. 2015. “Experimental Identification of Structural Dynamics and Aeroelastic Properties of A Self-sensing Smart Composite Wing,” In: *Proceedings of the 10th International Workshop on Structural Health Monitoring*, Stanford, US.

5. Roy S., Lonkar K., Janapati V., Chang F-K. 2014. “A novel physics-based temperature compensation model for structural health monitoring using ultrasonic guided waves,” *Structural Health Monitoring.*, 13(3):321-342.

6. Kopsaftopoulos F., Nardari R., Li Y., Chang F-K. 2018. “A stochastic global identification framework for aerospace structures operating under varying flight states,” *Mechanical Systems and Signal Processing.*, 98:425-447.

7. Samanta B. 2004. “Gear fault detection using artificial neural networks and support vector machines with genetic algorithms,” *Mechanical Systems and Signal Processing.*, 18:625-644.

8. Shen Z., Chen X., Zhang X., He Z. 2012. “A novel intelligent gear fault diagnosis model based on EMD and multi-class TSVM,” *Measurement.*, 45(1):30-40.

9. Lei Y., He Z., Zi Y., Hu Q. 2007. “Fault diagnosis of rotating machinery based on multiple ANFIS combination with GAs,” *Mechanical Systems and Signal Processing.*, 21(5):2280-2294.

10. Leung F. H., Lam H., Ling S., Tam P. K. 2003. “Tuning of the structure and parameters of a neural network using an improved genetic algorithm,” *IEEE Transactions on Neural networks*., 14(1):79-88.

11. Hinton G. E., Salakhutdinov R. R. 2006. “Reducing the dimensionality of data with neural networks,” Science., 313(5786):504-507.